Supporting Information

High-Efficiency and UV-Stable Flexible Perovskite Solar Cells Enabled by an Alkaloid-Doped C_{60} Electron Transport Layers

Xiaolong He†, Cheng Liu†, Yi Yang, Yong Ding, Shuang Ma, Yunzhao Wu, Ye Tao, Xuepeng Liu, Molang Cai and Songyuan Dai**

(†These authors contributed equally to this work.)

State Key Laboratory of Alternate Electrical Power System with Renewable Energy Sources, North China Electric Power University, Beijing 102206, P. R. China
E-mail: dingy@ncepu.edu.cn; sydai@ncepu.edu.cn

Experimental Section

Device Fabrication: Fullerene (C_{60}) films were deposited on the clean fluorine-doped tin oxide (FTO) or flexible indium-doped tin oxide (ITO)/polyethylene terephthalate (PET) substrates by spin-coating a nearly saturated solution of 28 mM C_{60} (Alfa, 99.5%) dissolved in 1,2-dichlorobenzene with a speed of 2000 rpm for 30 s and annealed at 60°C for 5 min. 0.1 mM 1,8-diazabicyclo[5.4.0]undec-7-ene (DBU, Alfa, 99%) was added in the C_{60}/1,2-dichlorobenzene solution to fabricate the DBU doped C_{60} (DBU-C_{60}) films. To compare the stability between the C_{60}- and TiO_2-based devices, the reference TiO_2-based devices were fabricated using a compact TiO_2 (c-TiO_2) ETLs by spray method at 500°C as previous reported.[1] $FA_{0.85}MA_{0.15}PbI_{2.55}Br_{0.45}$ precursor solution was prepared of 1.35 M Pb^{2+} (PbI_2 and $PbBr_2$) in a mixed solvent of DMSO and DMF (v/v=1:4). Both of the molar ratios for PbI_2 (TCI, 99.99%)/$PbBr_2$ (TCI, 99.99%) and FAI (TCI, 98%)/MABr (TCI, 98%) were fixed at 0.85:0.15. The completely dissolved solution was spin coated onto ETLs in the nitrogen glovebox with the following procedure: first 1000 rpm for 10 s and second 5000 rpm for 30 s with ramps of 1000 and 2500 rpm·s^{-1}, respectively. 110 μL of chlorobenzene was rapidly dripped on the rotating substrates during the second spin-coating step 15 s before the end of the procedure. The transparent perovskite film was then heated at 100 °C for 1.5 hours. A spiro-OMeTAD (PLT, 98%)/ chlorobenzene solution (60 mM) with additives of 28 μL 4-tert-butylpyridine (TBP, Aldrich, 96%) and 17.5 μL Li-TFSI (Alfa, 98%)/acetonitrile (1.8 M) and 8μL FK209-cobalt(III)-TFSI (PLT, 98%)/acetonitrile (0.2 M) was spin coated on top of the active layer at 4000 rpm for 30 s. Finally, 80-nm-thick Au was deposited by thermal evaporation under high vacuum.

Device characterization: The *J-V* characteristics of the devices were measured with a Keithley 2400 sourcemeter equipped with a sunlight simulator (XES-300T1, SAN-EI Electric, AM 1.5), which was calibrated using a standard silicon reference cell. The J-V curves of all devices were measured by masking the active area with a metal mask of 0.09 cm^2 under a simulated AM 1.5G spectrum. EQE was characterized by an Enli Technology EQE measurement system with a dual xenon/quartz halogen light source. The absorption spectra were recorded using UV/Vis spectrometer (Shimadzu, UV-3600) in the 300-900 nm range. PL and TRPL were recorded with a laser confocal Raman spectrometer (Princeton Instruments, Acton Standard Series SP-2558) and a 485 nm laser (PicoQuant LDH-P-C-485, 0.4 mW

with a 1% optical density filter) using a home-built confocal microscope. XRD spectra were performed with a Rigaku SmartLab SE X-ray diffractometer.

Table S1 Photovoltaic parameters of PSCs fabricated with C_{60} ETLs with different concentration of DBU dopant measured under AM1.5 illumination.

DBU concentration	J_{sc} (mA·cm^{-2})	V_{oc} (V)	*FF* (%)	*PCE* (%)
0.000 mM	23.34	1.00	75.13	17.54
0.025 mM	23.29	1.02	75.76	18.00
0.050 mM	23.51	1.05	75.43	18.62
0.075 mM	23.42	1.08	76.37	19.32
0.100 mM	23.49	1.10	76.62	19.80
0.125 mM	23.53	1.10	75.13	19.45
0.150 mM	23.28	1.09	73.46	18.64

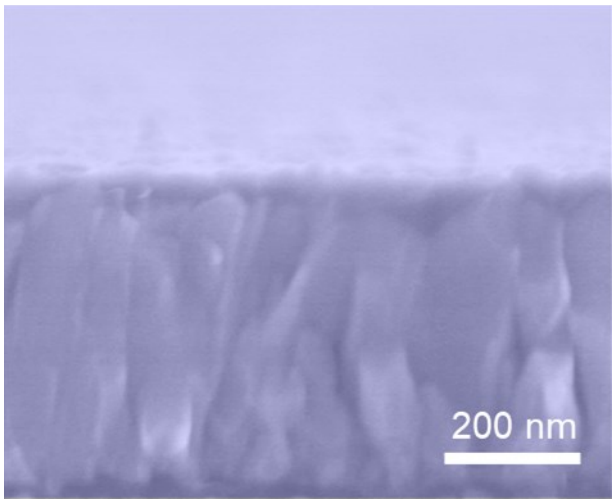

Fig. S1 Cross-section SEM of the C_{60} films. Scale bar, 200 nm.

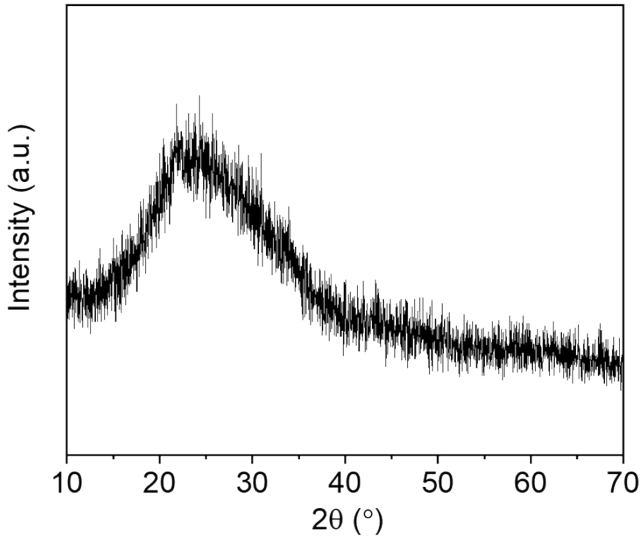

Fig. S2 XRD pattern of the C_{60} films.

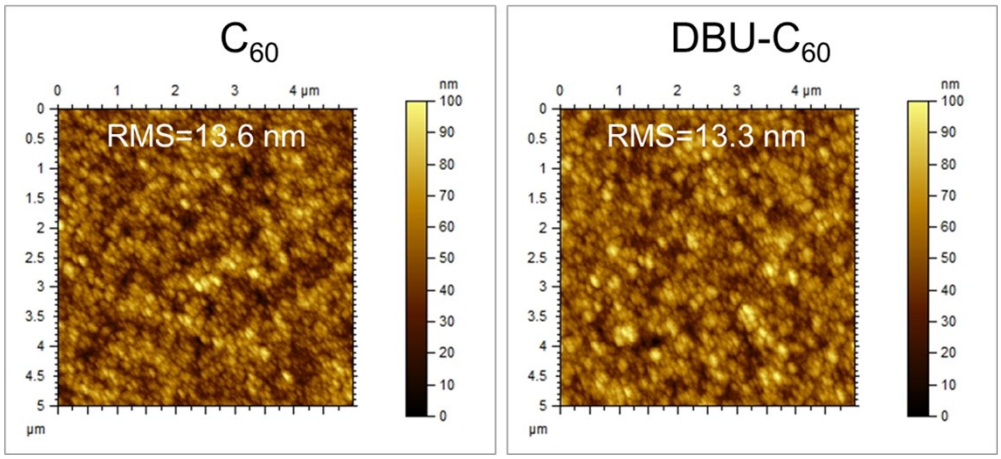

Fig. S3 Atomic force microscopy (AFM) images of the C_{60} and DBU-C_{60} films on the FTO substrates.

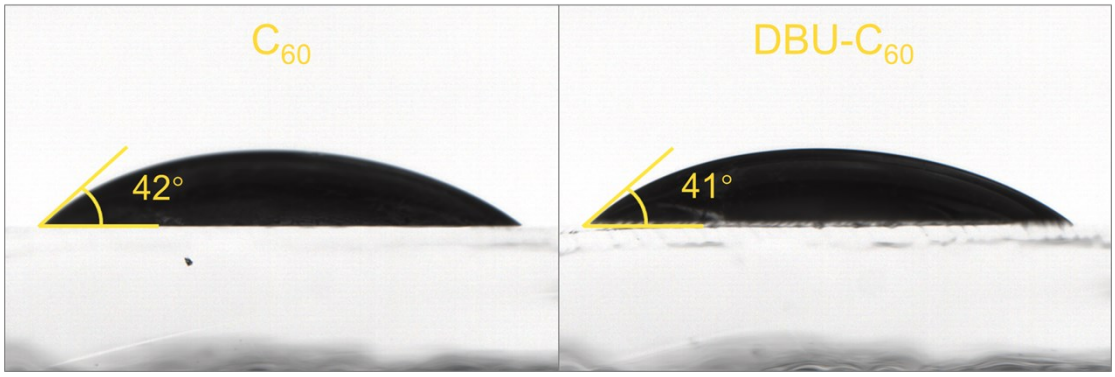

Fig. S4 Perovskite precursor contact angles of (c) C_{60} and (d) DBU-C_{60} substrates.

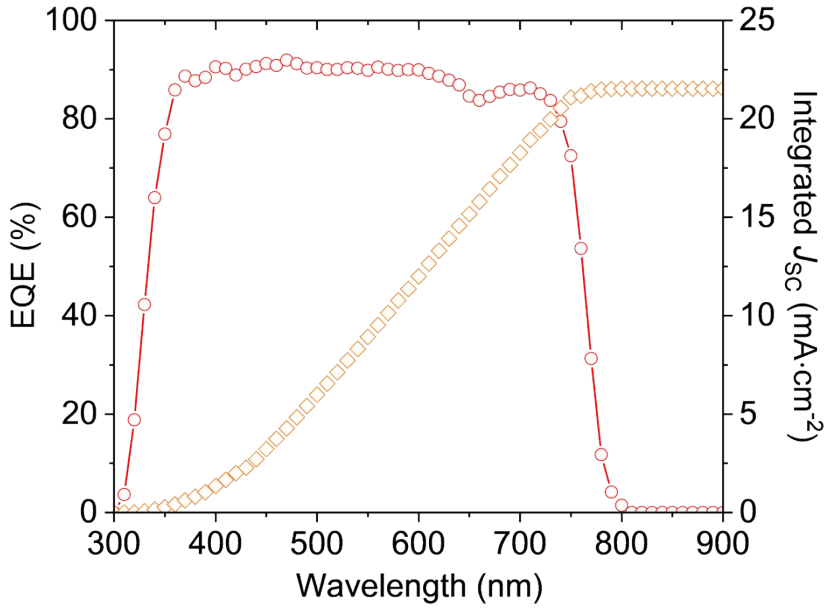

Fig. S5 External quantum efficiency (EQE) spectrum of the DBU-C_{60}-based PSC and the integrated short-circuit current density.

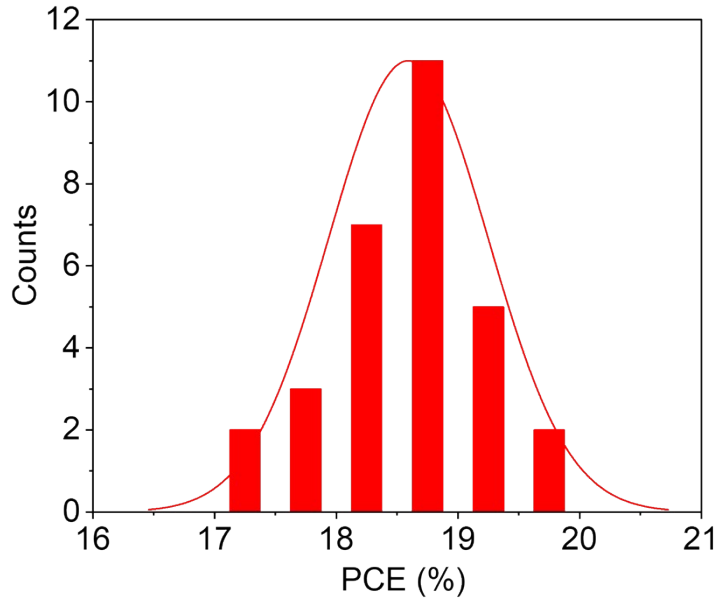

Fig. S6 Device performance distribution for 30 devices with DBU-C_{60} ETLs, the curve represents the Gaussian function of the histogram.

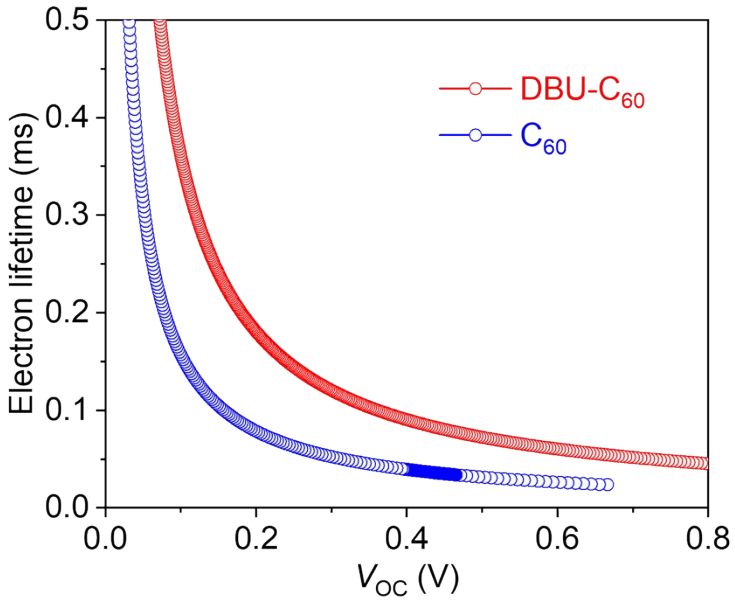

Fig. S7 The calculated electron lifetimes of the planner PSCs with C_{60} and DBU-C_{60} ETLs.

[1] Y. Yang, H. Peng, C. Liu, Z. Arain, Y. Ding, S. Ma, X. Liu, T. Hayat, A. Alsaedi, S. Dai, *J. Mater. Chem. A* **2019**, 7, 6450.